

Receptor-selective interleukin-4 mutein attenuates laser-induced choroidal neovascularization through the regulation of macrophage polarization in mice

LIMO GAO¹, WENMIN JIANG¹, HAIYING LIU², ZHIHENG CHEN³ and YANHUI LIN³

¹Department of Ophthalmology, The Second Xiangya Hospital, Central South University, Changsha, Hunan 410011;

²Hunan University of Finance and Economics, Changsha, Hunan 410205; ³Health Management Center, The Third Xiangya Hospital, Central South University, Changsha, Hunan 410013, P.R. China

Received January 26, 2020; Accepted May 4, 2021

DOI: 10.3892/etm.2021.10801

Abstract. Macrophage polarization has been recognized as an important inflammatory regulator in choroidal neovascularization (CNV). However, the mechanisms regulating macrophage activation and polarization, as well as their effects on angiogenesis and CNV, have not yet been elucidated. IL-4 is implicated in macrophage activation and exerts different functions in various diseases through several receptors. In the current study, the effect of IL-4 muteins on CNV was investigated *in vivo*. CNV was induced by laser coagulation in wild type mice. IL-4 muteins were recombined into adenoviruses and injected into mice via the tail vein. To evaluate CNV, fluorescein fundus angiography and optical coherence tomography were performed on day 7 after coagulation. Quantitative PCR, western blotting and immunofluorescence staining were used to assess the levels of inflammatory markers. AdIL-4/Q116E, an adenovirus-expressed recombinant IL-4 mutein, selectively activated macrophages, alleviated laser-induced CNV in mice with reduced expression of M2 macrophages and increased the expression of M1 macrophages. Furthermore, the expression of monocyte to macrophage differentiation-associated and delta-like 4 (Dlil4) in CNV lesions was upregulated. Employing

AdIL-4/Q116E, a IL-4RI-selective mutein, may serve as a new strategy for CNV therapy. Moreover, the results indicated that Dlil4 signaling served an important role in the regulation of macrophage polarization.

Introduction

IL-4 has been recognized as an important inflammatory regulatory cytokine that activates the differentiation of T cells into CD4⁺ T helper type 2 (Th2) subsets (1,2) and exerts an anti-inflammatory effect in macrophages (3). IL-4 functions in combination with two types of receptors: IL-4RI (type I IL-4 receptor), a heterodimer of IL-4R α and a common gamma-chain, and IL-4RII (type II IL-4 receptor), which consists of an IL-4R α and an IL-13R α 1 chain (4,5). A previous study indicated that IL-4 mediated immune responses in different types of cells by combining with different receptor sets and that IL-4 mutein exerted a Th2-deviation characteristic (6). In addition, this previous study demonstrated that the receptor-selective IL-4 mutein Q116E modulated the inflammatory phenotype of vascular cells and macrophages, and successfully attenuated atherosclerosis in a mouse model.

Choroidal neovascularization (CNV) is a major cause of reduced vision in patients with such diseases as age-related macular degeneration (AMD) and pathologic myopia (7). CNV may invade the subretinal space and cause pathological consequences, including retinal edema, detachment and hemorrhage (8). The causative factors that trigger CNV formation and the cascade of events during the pathogenesis of CNV have not been fully elucidated. However, progressive inflammatory event cascades and macrophage infiltration are widely considered to contribute to CNV (8). Zandi *et al* (9) reported that M1 macrophages were dominant in dry AMD, and that M2 macrophages enhanced CNV. Moreover, two types of macrophages can be found in CNV lesion sites of the patient at the same time (10). M2 macrophages upregulate the expression of vascular endothelial growth factor (VEGF) and promote neovascularization (11,12). Further studies have shown that the polarization of M2 macrophages was induced by exogenous stimulators inside the eyes, and intravitreal injection of M2 macrophages induced CNV (9,13). These

Correspondence to: Dr Yanhui Lin, Health Management Center, The Third Xiangya Hospital, Central South University, 138 Tongzipo Road, Changsha, Hunan 410013, P.R. China
E-mail: linyanhui1979@hotmail.com

Abbreviations: CNV, choroidal neovascularization; Th2, T helper type 2; Dlil1, delta-like 1; Dlil4, delta-like 4; AMD, age-related macular degeneration; VEGF, vascular endothelial growth factor; MMD, monocyte to macrophage differentiation-associated; FFA, fluorescein fundus angiography; OCT, optical coherence tomography; AdIL-4, adenovirus IL-4; AdIL-4 WT, adenovirus IL-4 wild type

Key words: IL-4, macrophage polarization, choroidal neovascularization, delta-like 4, mouse, animal experiments

studies have confirmed that the activation, aggregation and inflammatory factor release of macrophages are closely related to the occurrence and development of CNV. Different types of polarized macrophages play opposite roles: M1 macrophages are related to dry AMD, and M2 macrophages induce the occurrence of CNV (9). To date, there is no strategy put in place to regulate the polarization of macrophages to affect the formation of CNV.

To explore the therapeutic potential of IL-4-mediated immune responses in CNV, the present study investigated the effects of two receptor-selective IL-4 muteins on laser-induced CNV in mice. Single mutant IL-4/Q116E acted as an IL-4RI-specific agonist without activation of IL-4RII, and double mutant IL-4/Q116E/Y120D acted as an antagonist of IL-4RI and IL-4RII, as proven in a previous study (6). The present study hypothesized that IL-4 and its muteins can modulate the inflammatory phenotypes of macrophages through different receptors, and will affect CNV in a mouse model.

Materials and methods

Experimental animals. A total of 84 male 8-week-old C57BL/6 mice (18–20 g) (Cyagen Biosciences, Inc.) were used in the present study. Mice were bred under standard conditions (humidity, 55%; room temperature, 23±1°C; and 12-h dark-light cycle) with free access to chow and water. The study protocol was reviewed and approved by the Animal Care and Use Committees of the Third Xiangya Hospital of Central South University (Changsha, China).

Pre-experimental protocol for the establishment of a laser-induced CNV mouse model. Mice were anesthetized with intraperitoneal injection of ketamine (100 mg/kg) and xylazine (10 mg/kg). Pupils were then dilated with a drop of 1% tropicamide (Wuhan Wujing Medicine, Co., Ltd.). One eye of each mouse was left untreated as a control, and the other eye was irradiated with a 532-nm laser (integrated radiotherapy imaging system; 75 µm spot size; 0.1 sec interval; 0.1 sec duration; 100 mw power), which created 4–6 injury spots evenly distributed around the optic disc. The eyes were observed *in vivo* with a MICRON IV microscope (Phoenix Technology Group, LLC). A bubble formed at a laser-induced injury spot indicated the rupture of Bruch's membrane, which serves an important role in inducing neovascularization (7). Therefore, a total of 24 mice with eyes presenting bubbles formed at laser-induced injury spots were included in the study. Histological examination and immunofluorescence microscopy were performed on day 7 after laser coagulation. One mouse failed to wake up after laser photocoagulation, potentially because of an intolerance to ketamine and xylazine.

Histological examination and immunofluorescence microscopy. The mice were sacrificed by an overdose of pentobarbital (150 mg/kg), and death was confirmed by a lack of pulse. The eyeballs were fixed with 4% neutral formaldehyde solution (room temperature, 2 h). The corneas and lenses were removed from the eyes, and the remaining eyecups were then snap-frozen in Tissue-Tek® O.C.T.™ Compound (Sakura Finetek Japan Co., Ltd.). Serial cryostat sections (6-µm

thickness) of the eyecups were prepared and stained with H&E by standard methods.

For immunofluorescence microscopy, slides were blocked with PBS containing 1% BSA and 0.3% Triton X-100 for 30 min at room temperature, incubated with primary (4°C, overnight) and secondary (room temperature, 2 h) antibodies and counterstained with DAPI (cat. no. D8417; Sigma-Aldrich; Merck KGaA) for 10 min at room temperature. Slides were covered with coverslips, assessed and photographed by confocal laser scanning microscopy (Nikon Corporation). Primary antibodies included Alexa Fluor 647 anti-mouse CD206 (1:200; cat. no. 141712; BioLegend, Inc.), fluorescein isothiocyanate anti-mouse CD80 (1:200; cat. no. 11-0801; eBioscience; Thermo Fisher Scientific, Inc.), rat anti-mouse EGF-like module-containing mucin-like hormone receptor-like 1 (F4/80; 1:400; cat. no. 14-4801; eBioscience, Thermo Fisher Scientific, Inc.), goat anti-mouse delta-like 4 (Dll4; 1:400; cat. no. PA5-46974; Invitrogen; Thermo Fisher Scientific, Inc.) and goat anti-mouse CD31 (1:200; cat. no. AF3628; R&D Systems, Inc.). Secondary antibodies included donkey anti-goat IgG (1:500; Alexa Fluor 488; cat. no. CA11055S; Invitrogen; Thermo Fisher Scientific, Inc.), goat anti-rat IgG-biotin (1:500; cat. no. BA-9400; Maravai LifeSciences) and donkey anti-mouse IgG (1:500; Alexa Fluor 488; cat. no. CA21202S; Invitrogen; Thermo Fisher Scientific, Inc.). Cells with CD68-positive signals were identified as M1 macrophages, while cells with CD206-positive signals were identified as M2 macrophages (11).

Construction and *in vivo* transfection of recombinant IL-4-expressing adenoviruses. Adenovirus vectors expressing murine IL-4 were constructed as previously described (6). Briefly, the sequence of murine IL-4 in pcDNA3.1 (Thermo Fisher Scientific, Inc.) was subcloned into the shuttle vector pCMVAdvLink1 (Thermo Fisher Scientific, Inc.), and then co-transfected with the human adenovirus mutant *dl7001* into AD293 cells (Agilent Technologies, Inc.) to generate an adenovirus-expressed IL-4 wild-type (WT) vector, AdIL-4/Q116E (adenovirus-expressed IL-4, with Q116E mutation) and AdIL-4/Q116D/Y119D (adenovirus-expressed IL-4, with Q116D and Y119D mutations) vectors by homologous recombination. AdLacZ (adenovirus-expressed β-galactosidase) vector was used as a control in each experiment. For each mouse, 1×10⁸ plaque forming units of adenovirus vectors were diluted in 0.1 ml PBS and injected into the tail vein. For the CNV study, mice were injected with recombinant adenovirus vectors (n=3 for each condition) and then received laser treatment 1 day later. At day 7 after laser coagulation, the tissue samples were collected for use. Secreted IL-4 protein in the serum was measured by ELISA (cat. no. S4050; R&D Systems, Inc.) according to the manufacturer's instructions. IL-4 protein (~2–3 ng/ml) was detected 7 days after adenovirus infection (Fig. S1), indicating comparable IL-4 concentrations in the serum through adenovirus injection. Fluorescein fundus angiography (FFA) and optical coherence tomography (OCT). Mice were anesthetized with an intraperitoneal injection of ketamine (100 mg/kg) and xylazine (10 mg/kg), and the pupils were dilated with a drop of 1% tropicamide. Then, FFA and OCT were performed on both eyes of each

Table I. Sequences of primers for reverse transcription-quantitative PCR.

| Mouse gene | Forward primer (5'-3') | Reverse primer (5'-3') |
|----------------|-------------------------|---------------------------|
| <i>CD68</i> | GCTACATGGCGGTGGAGTACAA | ATGATGAGAGGCCAGCAAGATGG |
| <i>CD80</i> | TATTGCTGCCTTGCCGTTACA | AACAGATTCTGGTCCCCTTGA |
| <i>Arg-1</i> | AGACAGCAGAGGAGGTGAAGAG | CGAAGCAAGCCAAGGTTAAAG |
| <i>YM-1</i> | TCACAGGTCTGGCAATTCTTCTG | TGCATTCCAGCAAAGGCATAC |
| <i>MMD</i> | TGGATCAATGCGGTTTCAGGA | GCAATTGGCAGCATGTTTCGTAG |
| <i>Dll1</i> | GACGCTGAGGGGTATGTGATG | CTTGAGGCATACGCGAAAGAAGGTC |
| <i>Dll4</i> | GGGCACCTACTGTGAACTCC | GCTGCCCCACAAAGCCATAAG |
| <i>β-actin</i> | CAGCCTTCCTTCTTGGGTAT | TGGCATAGAGGTCTTTACGG |

Arg-1, arginase 1; Dll1, delta-like 1; Dll4: delta-like 4; MMD, monocyte to macrophage differentiation associated.

mouse using a MICRON IV retinal imaging microscope (Phoenix Technology Group, LLC) 3 min after intraperitoneal injection of 2.5% fluorescein sodium (Guangzhou Baiyunshan Mingxing Pharmaceutical Co., Ltd.). All images were recorded within 5-8 min of injection. For images of FFA, the fluorescent leakage intensity was graded as follows: 1, normal; 2, nonperfusion; 3, slight leakage; 4, moderate leakage; and 5, obvious leakage. For the OCT data, the images were graded as follows: 1, normal; 2, subretinal hyperreflective material with nonfibrotic scar; 3, subretinal hyperreflective material with fibrotic scar; and 4, intraretinal fibrotic scar.

Western blotting. Whole protein extracts were isolated from isolated retinal pigment epithelium (RPE)-choroid tissues with RIPA buffer (Santa Cruz Biotechnology, Inc.) and were then quantified with Quick Start™ Bradford Protein Assay kit (Bio-Rad Laboratories, Inc.). Subsequently, 20 mg of protein extracts were resolved by 10% SDS-PAGE gel and transferred onto PVDF membranes (Immobilon™; Sigma-Aldrich; Merck KGaA). The membranes were blocked with 5% fat-free milk for 30 min at room temperature, probed for overnight at 4°C with rabbit polyclonal anti-Dll4 (1:200; Abcam), goat polyclonal anti-delta-like 1 (Dll1; 1:200; cat. no. ab85346, Abcam), goat polyclonal anti-CD80 (1:500; cat. no. AF740, R&D Systems, Inc.), rabbit polyclonal anti-CD206 (1:500, cat. no. ab64693, Abcam), rabbit monoclonal anti-monocyte to macrophage differentiation associated (MMD) (1:200; cat. no. ab173967, Abcam), anti-β-actin antibody (1:2,000; cat. no. AC-15; Sigma-Aldrich; Merck KGaA), and then incubated with peroxidase-conjugated anti-rabbit-IgG (cat. no. A21020) or anti-goat-IgG (cat. no. A21030) (both 1:1,000; Abbkine Scientific Co., Ltd.) for 2 h at room temperature. The proteins were detected using ImmunoStar LD reagents (Wako Pure Chemical Industries, Ltd.) and visualized with a luminescent imager (Ez-Capture; ATTO Corporation).

RNA isolation and reverse transcription-quantitative PCR (RT-qPCR). Total RNA was isolated from isolated RPE-choroid tissues with TRIzol® reagent (Invitrogen; Thermo Fisher Scientific, Inc.). A total of 1 μg of extracted RNA per sample was reverse transcribed using a PrimeScript™ II Reverse Transcriptase kit (Takara Bio, Inc.) in a total volume of 20 μl, according to the manufacturer's instructions. Subsequently,

1 mg cDNA was used for qPCR with Fast™ SYBR-Green fluorescence dye (Applied Biosystems; Thermo Fisher Scientific, Inc.). Taq DNA polymerase was activated at 94°C for 10 min, followed by 40 cycles of 94°C for 20 sec and 65°C for 40 sec. Amplification reactions were performed in duplicate, fluorescence curves were analyzed with the included software of the StepOne real-time PCR system, and quantified using the 2^{-ΔΔC_q} method (14). All results were normalized to the expression of β-actin. The primer sequences used in the present study are listed in Table I.

Statistical analysis. The statistical analysis was performed using the SPSS 18.0 program (SPSS, Inc.). Image analysis was performed using ImageJ software (version 1.46; National Institutes of Health). All data are expressed as the mean ± SD. Mean values were compared with one-way ANOVA followed by Dunnett's test, categorical data were scaled according to the definition and compared using Kruskal-Wallis test. P<0.05 was considered to indicate a statistically significant difference. All experiments were repeated 3 times.

Results

Dll4 signaling activation in macrophages of CNV. The 12 eyes of 6 mice were included in the present study. The expression of Dll4 was observed not only in endothelial cells (CD31-positive cells; Fig. 1A and B) but also in macrophages (F4/80-positive cells; Fig. 1C and D). Dll4 was notably observed in endothelial cells (CD31-positive cells) of the outer and inner plexiform layers, not only in untreated eyes but also in laser-coagulated eyes. For macrophages (F4/80-positive cells), a low level of Dll4 expression was detected in the neuronal retina layer of untreated eyes, but the expression of Dll4 was notably increased in the neuronal retina layer of laser-coagulated eyes.

Polarization shift of M2 macrophages in laser-coagulated eyes. No difference was identified in the number of M1 macrophages (CD80-positive cells) before and 7 days after laser coagulation (Fig. 2A, B and E). Meanwhile, the number of M2 macrophages (CD206-positive cells) was significantly increased at 7 days after laser coagulation compared with that before laser coagulation (Fig. 2C-E), indicating a shift in macrophage polarization in eyes subjected to laser coagulation.

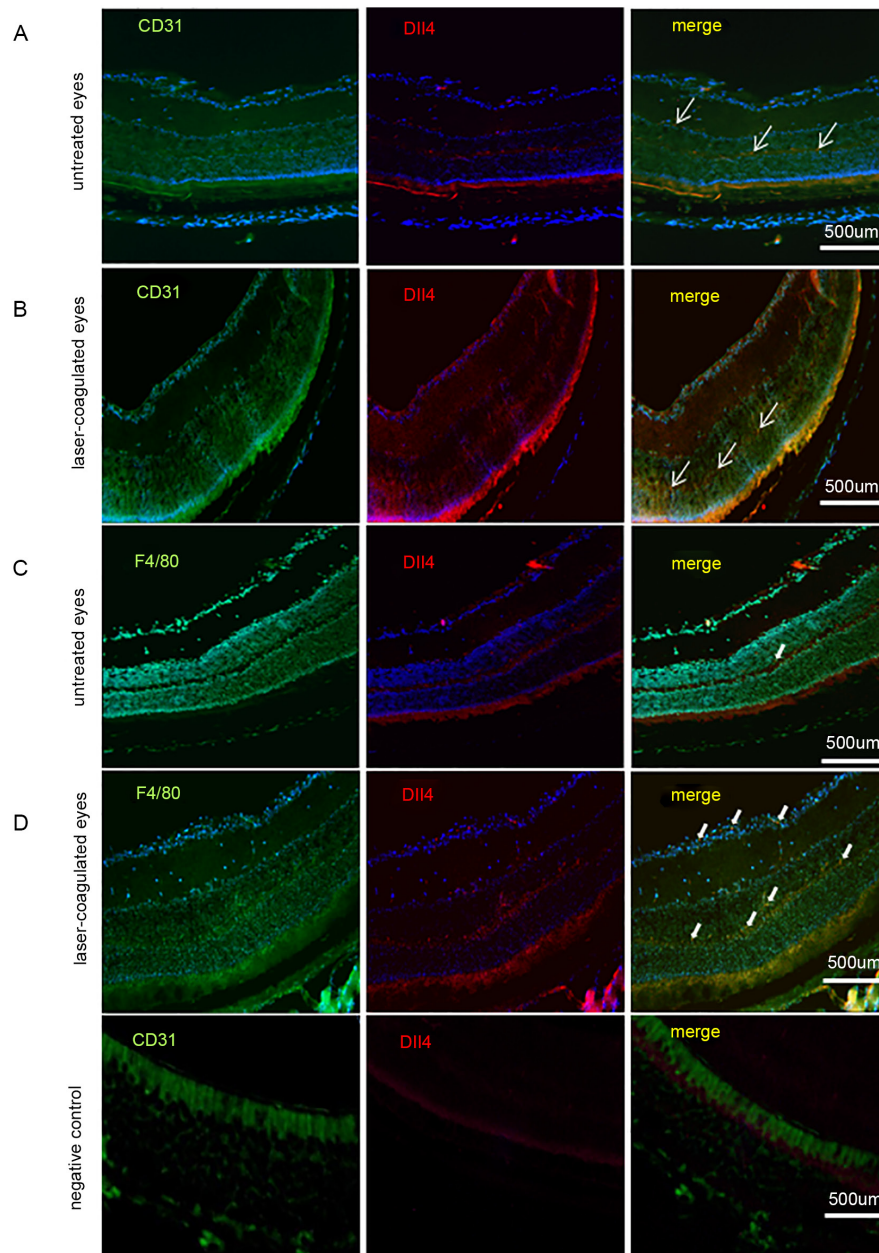


Figure 1. Expression of Dll4 in the retinal tissues of mice with laser-induced lesions was observed under an immunofluorescence microscope. One eye of each C57BL/6 mouse was exposed to a laser to induce CNV, and the other eye was left untreated. Eyecups were collected on day 7 after laser treatment. (A and B; thin white arrows) The expression of Dll4 in the endothelial cells was similar between untreated and laser-coagulated eyes. (C and D; thick white arrows) The expression level of Dll4 in macrophages was notably increased in laser-coagulated eyes compared with untreated eyes. Each experiment was repeated three times (n=3 mice per group). Scale bar, 500 μ m. CNV, choroidal neovascularization; Dll4, delta-like 4.

IL-4/Q116E attenuates laser-induced CNV in mice. Fundus images indicated a marked laser lesion around the optic disc in laser-coagulated eyes (Fig. 3A). Histological examination revealed that the retina was disordered in laser-coagulated eyes compared to untreated eyes (Fig. S2). The structure of the retinal neuronal layer was disrupted and unclear in laser-coagulated eyes compared with untreated eyes. AdIL-4/LacZ-injected and AdIL-4/WT-injected mice had the most severe laser-induced retinal injury, in which the retinal nerve fiber layer, inner nuclear layer and outer nuclear layer could not be distinguished (Fig. 3A). Furthermore, FFA revealed notable fluorescence leakage in the laser-induced retinal lesions of AdLacZ-injected mice and low levels of

fluorescence leakage in other AdIL-4 vector-infected mice, suggesting the establishment of CNV (Fig. 3A and C). OCT images showed disruptions in a highly reflective layer corresponding to the RPE and choriocapillaris in the laser-induced retinal lesions of AdLacZ-, AdIL-4/WT- and AdIL-4/Q116D/Y119D-infected mice, but not in AdIL-4/Q116E-infected mice (Fig. 3A and B).

IL-4/Q116E exerts an immunomodulatory effect in mice. The protein expression of CD80 was increased in both AdIL-4/Q116E- and AdIL-4/Q116E/Y119D-injected laser-coagulated eyes, whereas the expression of CD206 was decreased (Fig. 4A). Consistent with the results of western

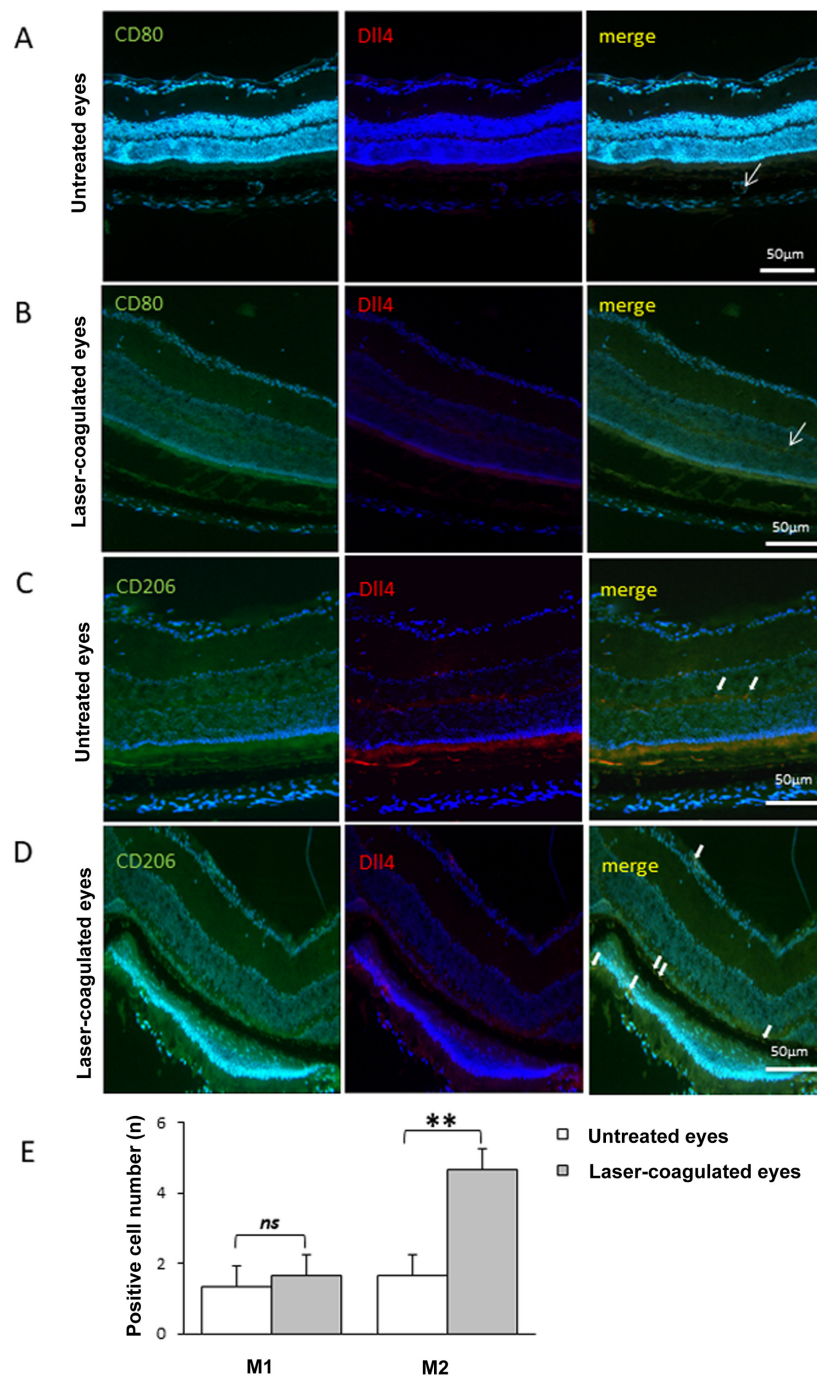


Figure 2. Distribution of M1 and M2 macrophages with Dll4 expression in laser-induced CNV observed under an immunofluorescence microscope. One eye of each C57BL/6 mouse was exposed to a laser to induce CNV, and the other eye was left untreated. Eyecups were collected on day 7 after laser coagulation. (A and B; thin white arrows) Dll4-positive M1 macrophages were marked by double staining for CD80 (green) and Dll4 (red). (C and D; thick white arrows) Dll4-positive M2 macrophages in cryosections of the CNV lesion were found expressed at low levels either untreated or after laser coagulation. Dll4-positive M2 macrophages were marked by double staining for CD206 (green) and Dll4 (red). (E) Dll4-positive M2 macrophage number in cryosections of the CNV lesion was significantly increased after laser coagulation compared with untreated eyes. Each experiment was repeated three times. Data are expressed as the means \pm SD (n=3 mice per group). **P<0.01 as indicated. Scale bar, 50 μ m. CNV, choroidal neovascularization; Dll4, delta-like 4; ns, no significance.

blotting, compared with laser-coagulated eyes with the LacZ negative control, CD68 and CD80 mRNA expression levels were decreased in AdIL-4/WT-infected laser-coagulated eyes and increased in AdIL-4/Q116E-infected laser-coagulated eyes (Fig. 4B). Compared with laser-coagulated eyes treated with the AdLZ negative control, arginase 1 (Arg-1) was down-regulated in AdIL-4/Q116E-infected laser-coagulated eyes, CD80 was upregulated in AdIL-4/Q116D/Y119D-infected

laser-coagulated eyes, and no difference in expression was observed for the chitinase-like protein YM-1 (Fig. 4B).

Taken together, these results suggested that IL-4 led to a polarization shift of M2/M1 macrophages in different adenovirus-transfected eyes.

IL-4/Q116E regulates the expression of MMD and Dll4. AdIL-4/Q116E injection in laser-coagulated eyes increased

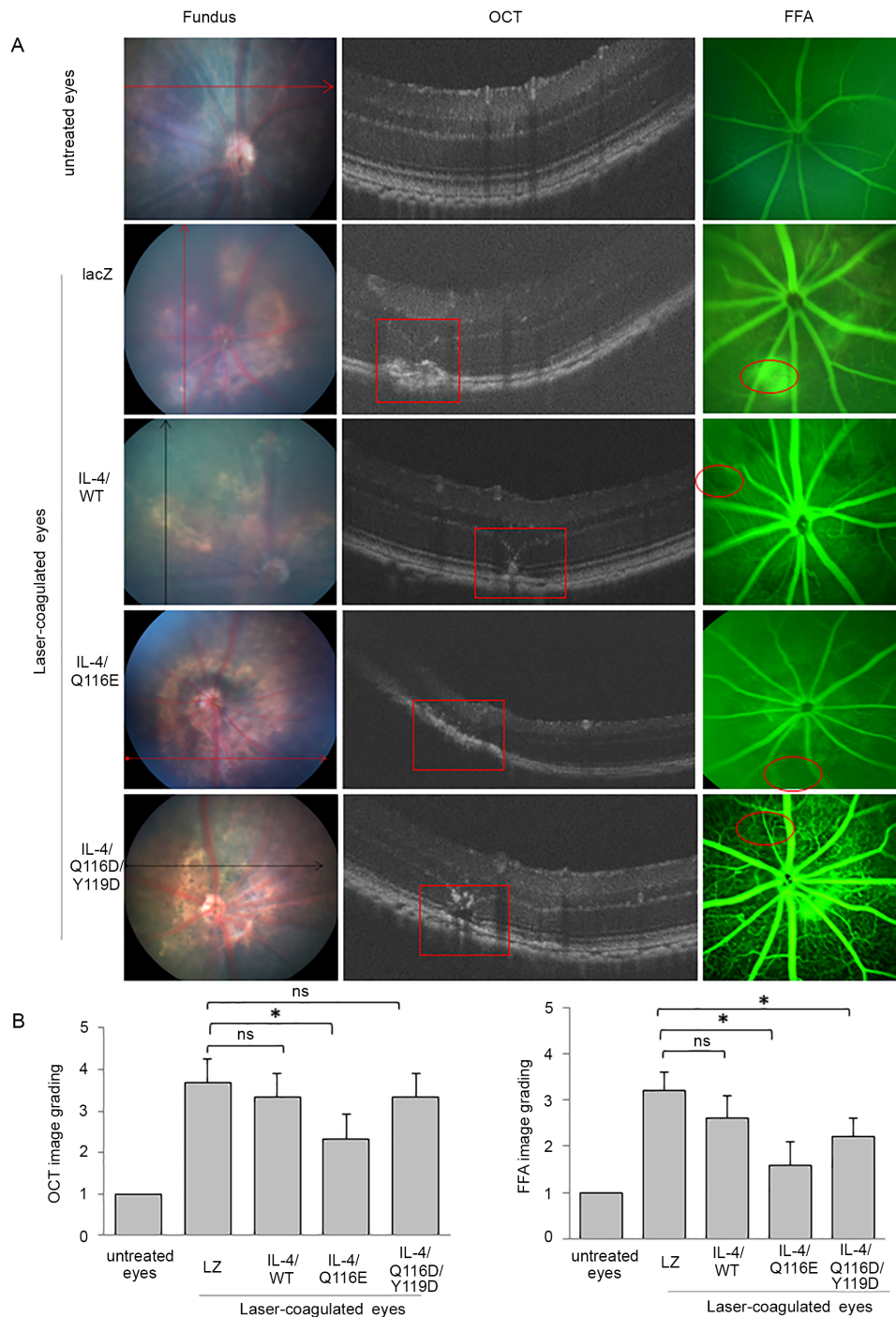


Figure 3. CNV induction through photocoagulation, and IL-4/Q116E attenuation of CNV in laser-induced mice. C57BL/6 mice were injected with the control vector AdLZ or the three recombinant IL-4 vectors and subsequently received laser coagulation 1 day later. On day 7 after laser coagulation, one eye of each mouse was removed. Fundus images, FFA and OCT of the laser-treated eyes of adenovirus-injected mice were performed at 3 min after intraperitoneal injection of 2.5% fluorescein sodium. (A) Untreated eyes revealed normal images without laser injury spots, with clear layers and no fluorescence leakage. Laser-treated eyes exhibited laser injury spots (as indicated by arrows), retinal tomostructure (as indicated by red squares) and fluorescence leakage (as indicated by red circles) in the scanned area. All images were recorded within 5-8 min. (B) Image grading for OCT and FFA images was established. Data are expressed as the means \pm SD (n=3 mice per group). *P<0.05 as indicated. CNV, choroidal neovascularization; FFA, fluorescein fundus angiography; IL-4, adenovirus-expressed IL-4 vector; LacZ, adenovirus-expressed β -galactosidase; ns, no significance; OCT, optical coherence tomography; WT, wild-type.

the expression of MMD and Dll4 but did not affect the expression of Dll1 at the protein level (Fig. 5A). At the mRNA level, AdIL-4/Q116E increased the expression of MMD, Dll1 and Dll4 (Fig. 5B).

AdIL-4/Q116D/Y119D injection of laser-coagulated eyes increased the expression of Dll4 but did not affect the expression of MMD and Dll1 at the protein level (Fig. 5A). At the

mRNA level, AdIL-4/Q116D/Y119D injection increased the expression levels of MMD and Dll1 but not Dll4 (Fig. 5B).

Discussion

The present study indicated that IL-4 muteins affected CNV development by modulating macrophage phenotypes. The IL-4

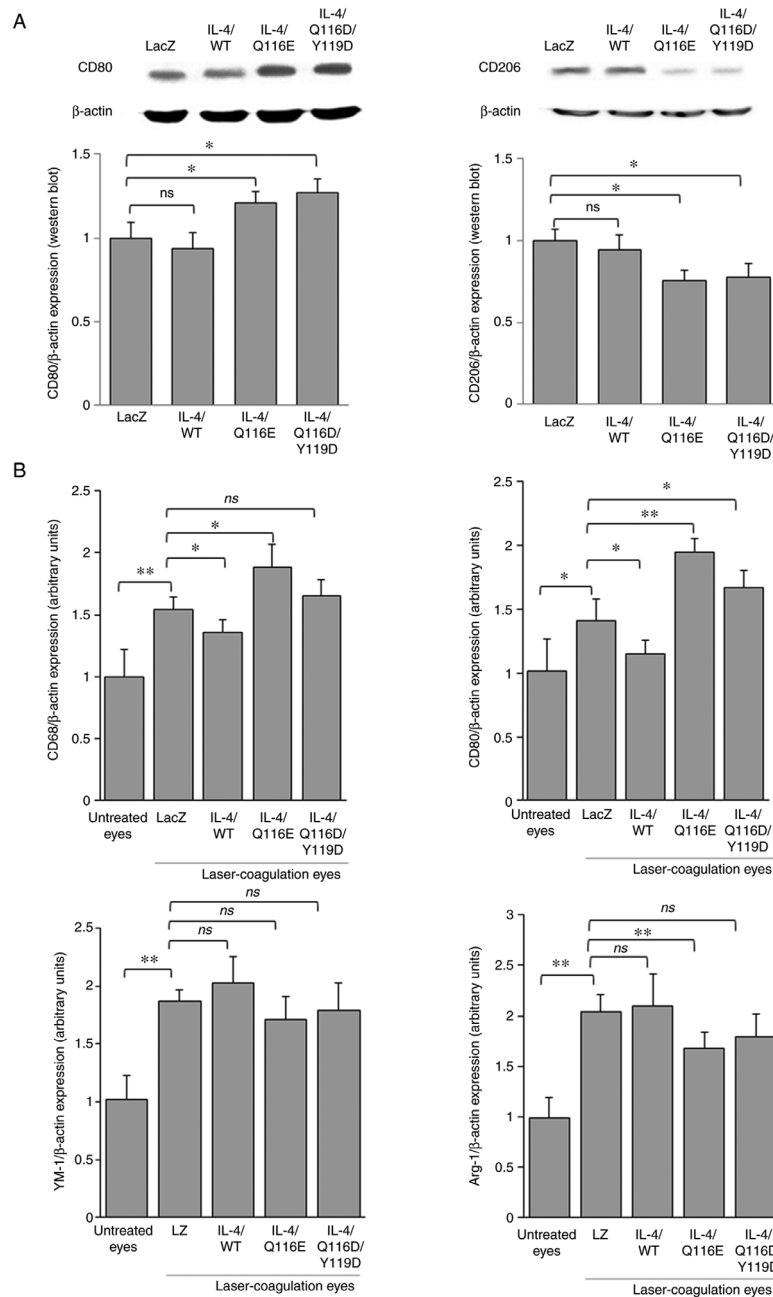


Figure 4. Distribution of M1 and M2 macrophages in RPE-choroid tissues of laser-induced CNV. RPE-choroid tissues were resected from mice exhibiting laser-induced CNV lesions. (A) The expression of CD80 and CD206 was determined by western blotting, with β -actin as a control. Each experiment was repeated three times. (B) Reverse transcription-quantitative PCR was performed, and the expression levels of CD68, CD80, Arg-1 and YM-1 were normalized to β -actin. Data are expressed as the mean \pm SD (n=3 mice per group). *P<0.05 and **P<0.01 as indicated. Arg-1, arginase 1; CNV, choroidal neovascularization; IL-4, adenovirus-expressed IL-4 vector; LacZ and LacZ, adenovirus-expressed β -galactosidase; ns, no significance; RPE, retinal pigment epithelium; WT, wild-type; YM-1, chitinase-like protein 3.

mutin IL-4/Q116E attenuated laser-induced CNV in mice. Furthermore, IL-4/Q116E not only remodeled the anatomical structure of the retina and choroid but also reduced vascular leakage according to OCT and FFA data.

Pre-experimental data indicated that not only endothelial cells but also macrophages participated in laser-induced retinal lesions. Additionally, M2 macrophages (CD206-positive cells) were increased after laser coagulation and M1 macrophages (CD80-positive cells) were not clearly increased compared with untreated eyes and laser-coagulated eyes. The results confirmed that M2 macrophages were dominant in laser-induced retinal lesions. A previous study

also reported that laser-induced retinal lesions are one of the causes of CNV (11). In addition, the investigation of the inflammatory factors in RPE-choroid tissue from mice infected with different AdvIL-4 vectors revealed that AdIL-4/Q116E led to the polarization shift of macrophages from the M2 to M1 phenotype; the expression levels of CD68 and CD80 were increased, and the expression level of Arg-1 was decreased. These results are in contradiction with those reported by another group (15), who found that macrophage infiltration accentuated neovascularization by a direct effect on endothelial cell proliferation in situations of inflammatory neovascularization. Our previous study reported that Th2

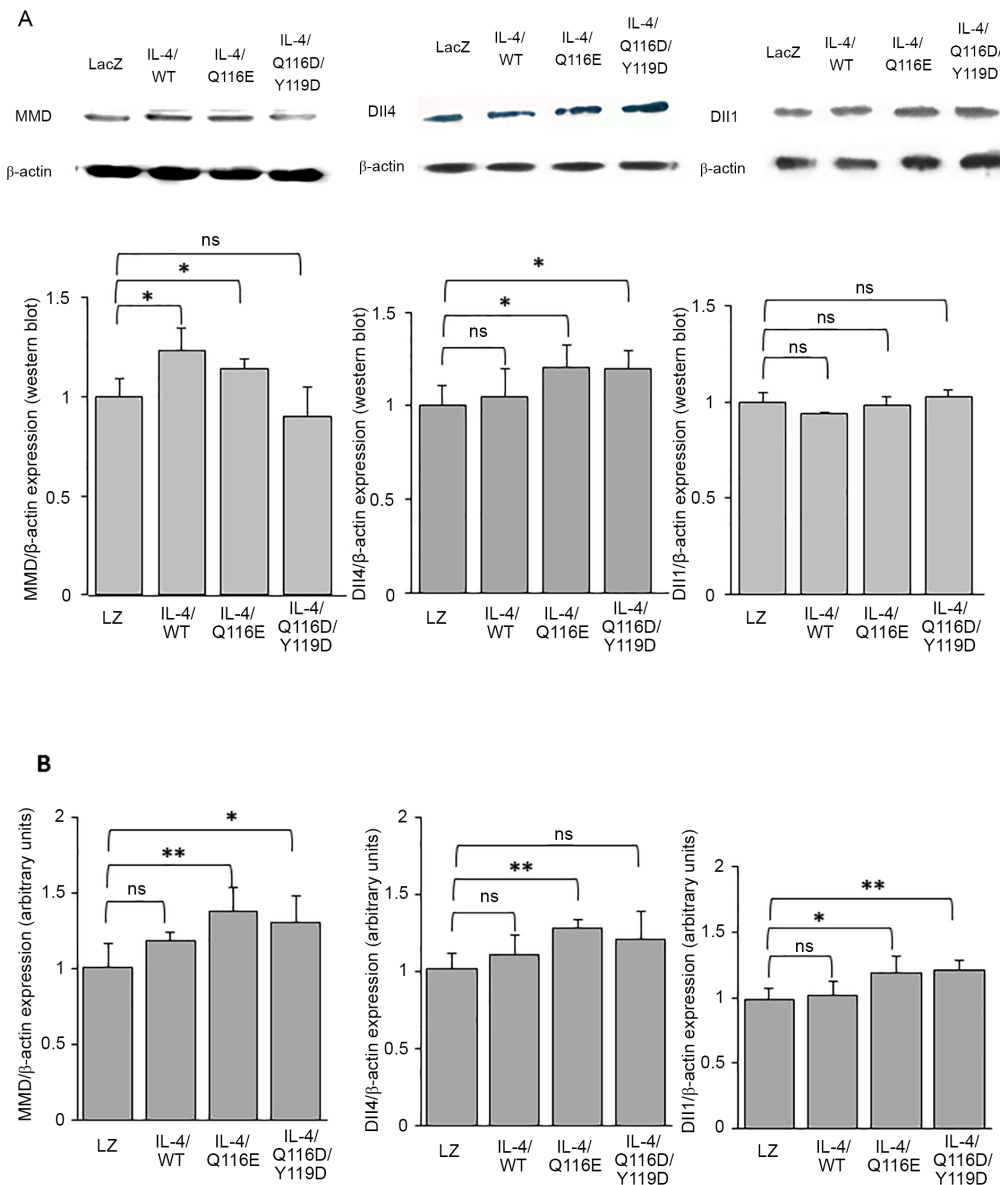


Figure 5. MMD-Dll4 pathway expression in RPE-choroid tissues of laser-induced CNV. RPE-choroid tissues were resected from mice exhibiting laser-induced CNV. (A) The expression of MMD, Dll1 and Dll4 was determined by western blotting, with β -actin as a control. Each experiment was repeated three times. Statistical analysis was performed using ImageJ software. (B) Reverse transcription-quantitative PCR was performed, and the expression of MMD, Dll4 and Dll1 was normalized to β -actin. Data are expressed as the mean \pm SD (n=3 mice per group). *P<0.05 and **P<0.01 as indicated. Dll1, delta-like 1; Dll4, delta-like 4; IL-4, adenovirus-expressed IL-4 vector; LacZ and LacZ, adenovirus-expressed β -galactosidase; MMD, monocyte to macrophage differentiation-associated; ns, no significance; RPE, retinal pigment epithelium; WT, wild-type.

deviation in splenocyte responses and reduced atherosclerotic area in AdvIL-4/Q116E-infected mice. Additionally, the results demonstrated that IL-4/Q116E served a diverse inflammatory role in different cell types. For example, IL-4/Q116E increased the expression level of vascular cell adhesion molecule 1 (VCAM-1) in endothelial cells and partially inhibited the effects of IL-4 on different macrophages (6). Therefore, it can be hypothesized that IL-4/Q116E has a cell-specific effect on inflammation, serving similar or opposite roles in different cell types. However, these findings are not sufficient to explain how IL-4/Q116E attenuates CNV. Other immune cells, such as lymphocytes, may serve an important role, as IL-4/Q116E regulates Th1/Th2 deviation, as our previous reports (6). Therefore, further experiments on local and systemic immune responses in CNV are required.

A previous study reported that Notch signaling serves a pivotal role in the inflammatory response and angiogenesis by regulating the polarization of macrophages. It also participates in the development of certain diseases, such as CNV (16). Dll4 is a ligand of Notch signaling that has the same function as VEGF (17). When the allele signaling molecule of Dll4 is deleted, it can cause vascular abnormalities at the embryonic stage, suggesting that Dll4 serves an important role in vascular development and homeostasis in the same manner as VEGF (17). The present study indicated that the expression level of Dll4 in the CNV model was significantly increased not only in the neuronal retina layer, but also in the subretinal area compared with its expression in untreated eyes. In addition, the present study reported that, similar to Dll4-positive endothelial cells, Dll4-positive macrophages also participated in CNV, which is

consistent with other studies (7,18). However, Camelo *et al* (15) hypothesized that Dll4 stimulated CNV through macrophages, as VEGF was upregulated after the overexpression of Dll4. In the same study, it was reported that the expression levels of IL-1 β , IL-6 and TNF- α were increased, which confirmed that overexpression of Dll4 stimulated macrophage shift to M1 polarization. These results are consistent with the present data.

To investigate the possible signaling pathway of IL-4 muteins, the expression levels of genes involved in Notch signaling in CNV were quantified. The results revealed that the expression levels of MMD and Dll4 were increased in RPE-choroid tissue obtained from IL-4/Q116E-infected mice. MMD was identified in 1995 by analyzing the molecular mechanism of macrophage maturation and was speculated to participate in the differentiation and functional process of macrophages (19). Subsequently, Liu *et al* (20) reported that MMD positively regulated the activation of ERK, protein kinase B and the production of TNF- α and nitric oxide in macrophages, which was consistent with the present data to some extent, where MMD upregulated the expression of M1 cytokine. Therefore, MMD may participate in the differentiation of macrophages and stimulate the secretion of cytokines from M1 macrophages. The present study reported that AdIL-4/Q116E stimulated M1-macrophage shift, including upregulation of CD68 and CD80 and downregulation of CD206 and Arg-1. However, there is no notable reason to certify that MMD is downstream of the Notch-Dll4 signaling pathway that affects macrophage polarization, as experiments with an MMD blocker were not performed in the present study. The present data reported the possibility that IL-4 mutein attenuated CNV by regulating macrophage polarization. It also demonstrated that Notch-Dll4-MMD could be a possible signaling pathway involved in these events. In future studies, it will be investigated if regulating the expression of Dll4 or MMD, such as MMD overexpression, or using a Dll4 blocker, could change the shift of macrophage polarization. Furthermore, future studies should identify the downstream signaling pathways involved, such as ERK, AKT and mitogen-activated protein kinase.

In summary, the present results demonstrated that IL-4/Q116E regulated the inflammatory response in laser-induced CNV, increased the expression of CD68 and CD80, decreased the expression of Arg-1 in RPE-choroid tissues and attenuated CNV development. The results suggested that targeting macrophage polarization and its inflammatory reaction may be a possible treatment strategy for CNV. Furthermore, the present results provide a foundation for further research investigating the MMD-Dll4 signaling pathway as a potential target of IL-4 muteins to treat CNV and other intraocular inflammatory disorders.

In conclusion, IL-4RI-selective mutein AdIL-4/Q116E regulated macrophage polarization and alleviated CNV.

Acknowledgements

Not applicable.

Funding

This study was supported in part by Grant-in-Aids for Young Scientists (grant nos. 2017JJ3465 and 2017JJ3473) from the Hunan Natural Science Foundation, P.R. China.

Availability of data and materials

All data generated or analyzed during this study are included in this published article.

Authors' contributions

LG was responsible for data curation, carrying out the study and writing (original draft). WJ was responsible for analyzing the data and ophthalmologic examination, and HL, for literature searching and analyzing the data. ZC was responsible for the study conception and design. YL contributed to study conception and supervision, as well as manuscript writing editing. LG and YL confirm the authenticity of all the raw data. All authors have read and approved the final manuscript.

Ethics approval and consent to participate

The study protocol was reviewed and approved by the Animal Care and Use Committees of the Third Xiangya Hospital, Central South University (Changsha, China).

Patient consent for publication

Not applicable.

Competing interests

The authors declare that they have no competing interests

References

1. Paul WE: Interleukin-4: A prototypic immunoregulatory lymphokine. *Blood* 77: 1859-1870, 1991.
2. Boothby M, Mora AL, Aronica MA, Youn J, Sheller JR, Goenka S and Stephenson L: IL-4 signaling, gene transcription regulation, and the control of effector T cells. *Immunol Res* 23: 179-191, 2001.
3. Hamilton TA, Ohmori Y and Tebo J: Regulation of chemokine expression by antiinflammatory cytokines. *Immunol Res* 25: 229-245, 2002.
4. Ramalingam TR, Pesce JT, Sheikh F, Cheever AW, Mentink-Kane MM, Wilson MS, Stevens S, Valenzuela DM, Murphy AJ, Yancopoulos GD, *et al*: Unique functions of the type II interleukin 4 receptor identified in mice lacking the interleukin 13 receptor alpha chain. *Nat Immunol* 9: 25-33, 2008.
5. LaPorte SL, Juo ZS, Vaclavikova J, Colf LA, Qi X, Heller NM, Keegan AD and Garcia KC: Molecular and structural basis of cytokine receptor pleiotropy in the interleukin 4/13 system. *Cell* 132: 259-272, 2008.
6. Lin Y, Chen Z and Kato S: Receptor-selective IL-4 mutein modulates inflammatory vascular cell phenotypes and attenuates atherogenesis in apolipoprotein E-knockout mice. *Exp Mol Pathol* 99: 116-127, 2015.
7. Dou GR, Li N, Chang TF, Zhang P, Gao X, Yan XC, Liang L, Han H and Wang YS: Myeloid-specific blockade of Notch signaling attenuates choroidal neovascularization through compromised macrophage infiltration and polarization in mice. *Sci Rep* 6: 28617, 2016.
8. Cherepanoff S, McMenamin P, Gillies MC, Kettle E and Sarks SH: Bruch's membrane and choroidal macrophages in early and advanced age-related macular degeneration. *Br J Ophthalmol* 94: 918-925, 2010.
9. Zandi S, Nakao S, Chun KH, Fiorina P, Sun D, Arita R, Zhao M, Kim E, Schueller O, Campbell S, *et al*: ROCK-isoform-specific polarization of macrophages associated with age-related macular degeneration. *Cell Rep* 10: 1173-1186, 2015.
10. Yang Y, Liu F, Tang M, Yuan M, Hu A, Zhan Z, Li Z, Li J, Ding X and Lu L: Macrophage polarization in experimental and clinical choroidal neovascularization. *Sci Rep* 6: 30933, 2016.

11. Zhou Y, Yoshida S, Kubo Y, Yoshimura T, Kobayashi Y, Nakama T, Yamaguchi M, Ishikawa K, Oshima Y and Ishibashi T: Different distributions of M1 and M2 macrophages in a mouse model of laser-induced choroidal neovascularization. *Mol Med Rep* 15: 3949-3956, 2017.
12. Jetten N, Verbruggen S, Gijbels MJ, Post MJ, De Winther MP and Donners MM: Anti-inflammatory M2, but not pro-inflammatory M1 macrophages promote angiogenesis in vivo. *Angiogenesis* 17: 109-118, 2014.
13. Zhang P, Wang H, Luo X, Liu H, Lu B, Li T, Yang S, Gu Q, Li B, Wang F, *et al*: MicroRNA-155 inhibits polarization of macrophages to M2-type and suppresses choroidal neovascularization. *Inflammation* 41: 143-153, 2018.
14. Livak KJ and Schmittgen TD: Analysis of relative gene expression data using real-time quantitative PCR and the $2(-\Delta\Delta C(T))$ Method. *Methods* 25: 402-408, 2001.
15. Camelo S, Raoul W, Lavalette S, Calippe B, Cristofaro B, Levy O, Houssier M, Sulpice E, Jonet L, Klein C, *et al*: Delta-like 4 inhibits choroidal neovascularization despite opposing effects on vascular endothelium and macrophages. *Angiogenesis* 15: 609-622, 2012.
16. Michelucci A, Heurtaux T, Grandbarbe L, Morga E and Heuschling P: Characterization of the microglial phenotype under specific pro inflammatory and anti inflammatory conditions: Effects of oligomeric and fibrillar amyloid beta. *J Neuroimmunol* 210: 3-12, 2009.
17. Wu ZQ, Rowe RG, Lim KC, Lin Y, Willis A, Tang Y, Li XY, Nor JE, Maillard I and Weiss SJ: A Snail1/Notch1 signalling axis controls embryonic vascular development. *Nat Commun* 5: 3998, 2014.
18. Yan X, Yang Z, Chen Y, Li N, Wang L, Dou G, Liu Y, Duan J, Feng L, Deng S, *et al*: Endothelial cells-targeted soluble human Delta-like 4 suppresses both physiological and pathological ocular angiogenesis. *Sci China Life Sci* 58: 425-431, 2015.
19. Rehli M, Krause SW, Schwarzfischer L, Kreutz M and Andreesen R: Molecular cloning of a novel macrophage maturation-associated transcript encoding a protein with several potential transmembrane domains. *Biochem Biophys Res Commun* 217: 661-667, 1995.
20. Liu Q, Zheng J, Yin DD, Xiang J, He F, Wang YC, Liang L, Qin HY, Liu L, Liang YM, *et al*: Monocyte to macrophage differentiation-associated (MMD) positively regulates ERK and Akt activation and TNF- α and NO production in macrophages. *Mol Biol Rep* 39: 5643-5650, 2012.



This work is licensed under a Creative Commons Attribution-NonCommercial-NoDerivatives 4.0 International (CC BY-NC-ND 4.0) License.